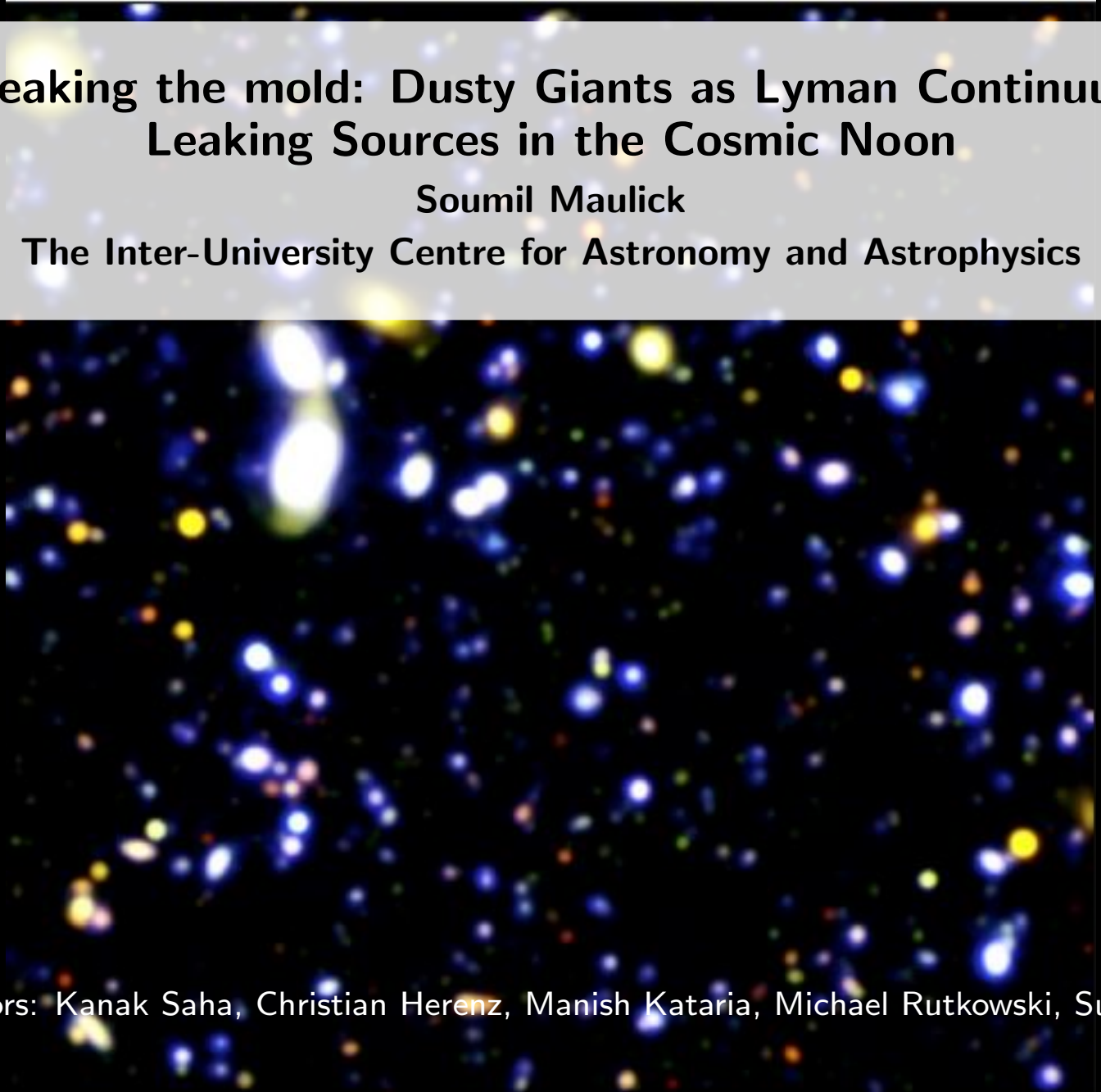

Breaking the mold: Dusty Giants as Lyman Continuum Leaking Sources in the Cosmic Noon

Soumil Maulick

The Inter-University Centre for Astronomy and Astrophysics

Collaborators: Kanak Saha, Christian Herenz, Manish Kataria, Michael Rutkowski, Suraj Dhiwar

Massive dusty galaxies: Poor candidates for LyC escape?

- Inefficient clearing of neutral gas and/or increased dust attenuation (Ma+2020, Rosdahl+2022).

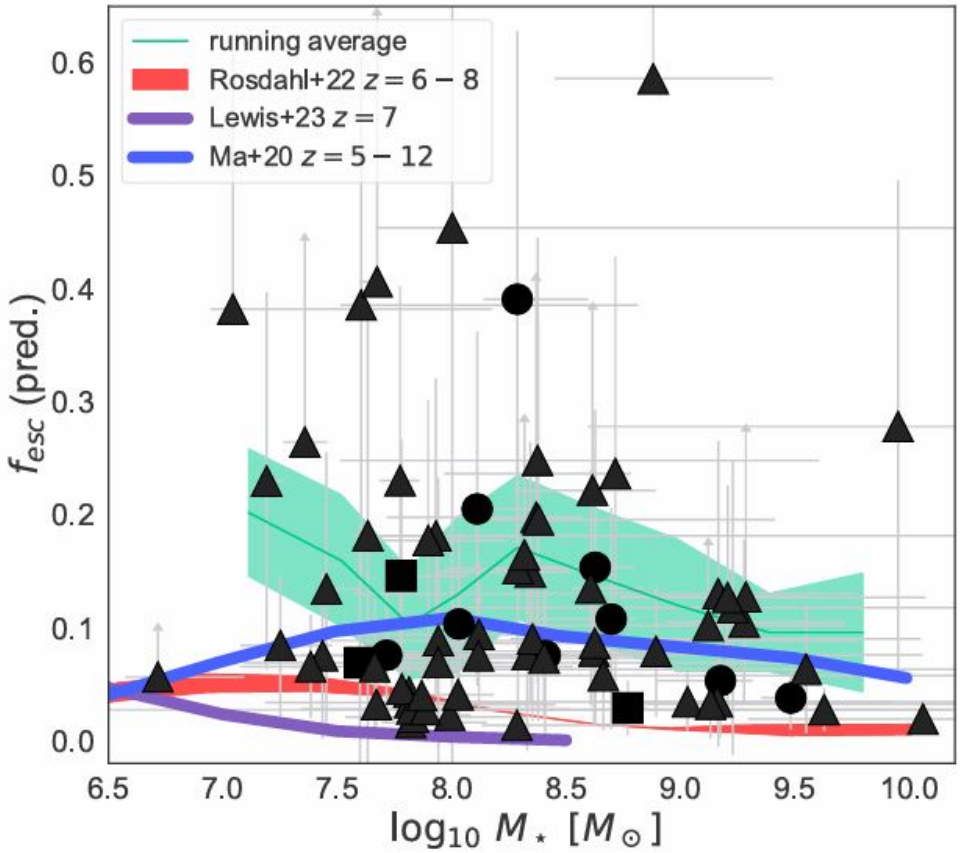

Mascia+2024

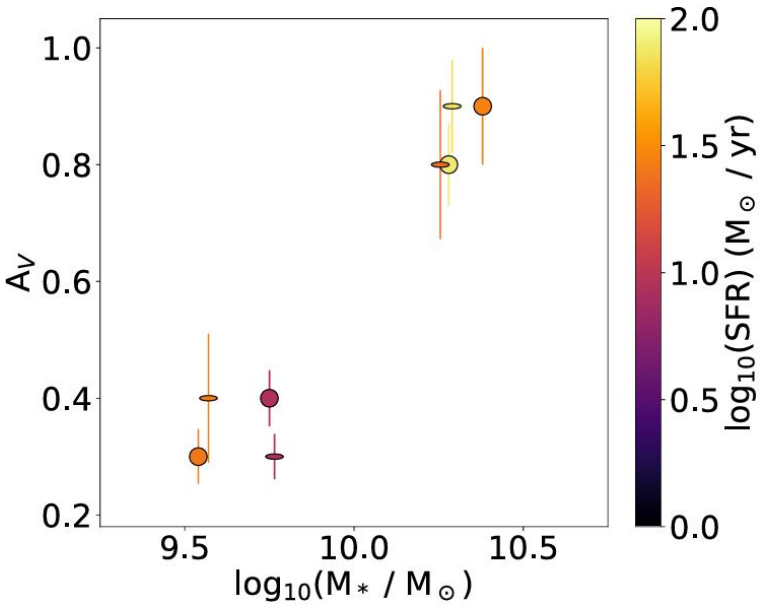

Lorenz+2023

- Few such LyC leakers have been detected at $z \sim 0.2 - 0.3$ (Wang+2019, Roy+2024) and at $z \sim 1$ (Maulick+2024a,b).

Emerging population of massive dusty LyC leakers

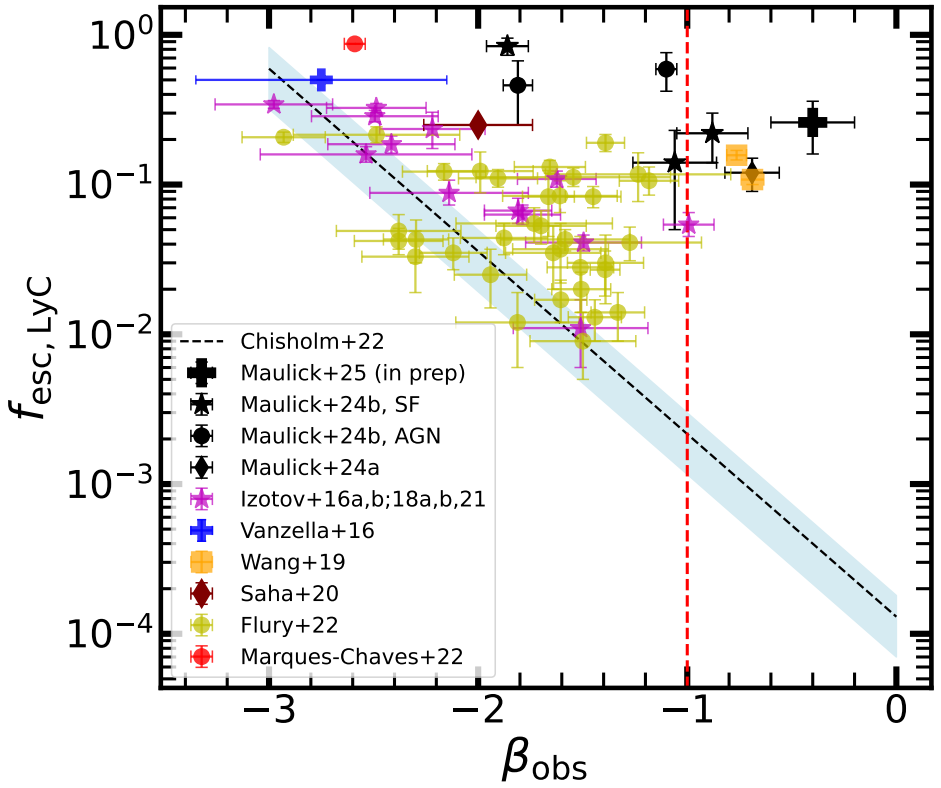

- Clumpiness may cause locally bluer $\beta_{\rm obs}$ than integrated values (Bolamperti+2023).

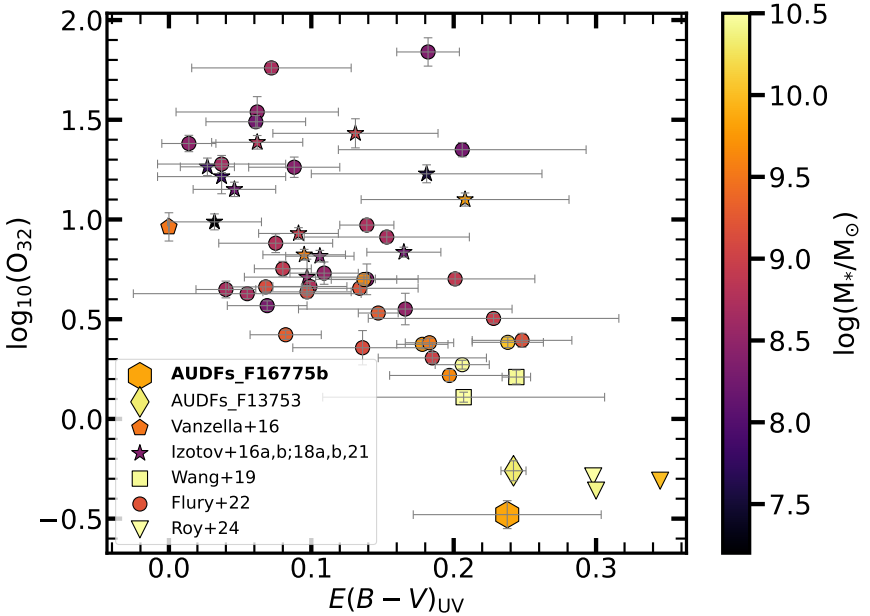

- Low ($\lesssim 1$) O32 values difficult to reconcile with density-bounded escape.
- Wang+2019 and Roy+2024 objects are compact and are [S II] deficient.

Case of LyC Leakage from an Evolved Spiral Galaxy at $z \sim 1.1$

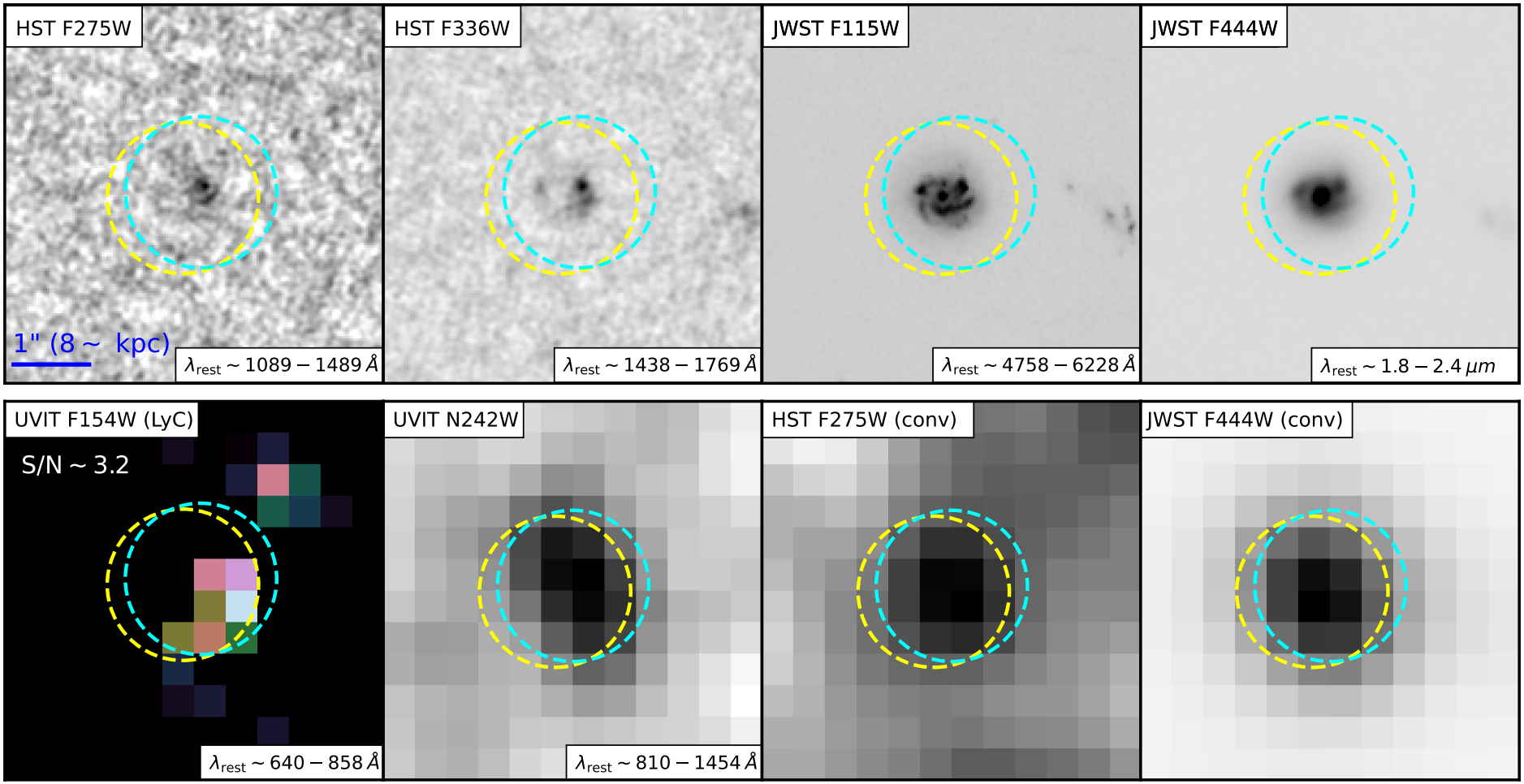

Stellar population and dust properties

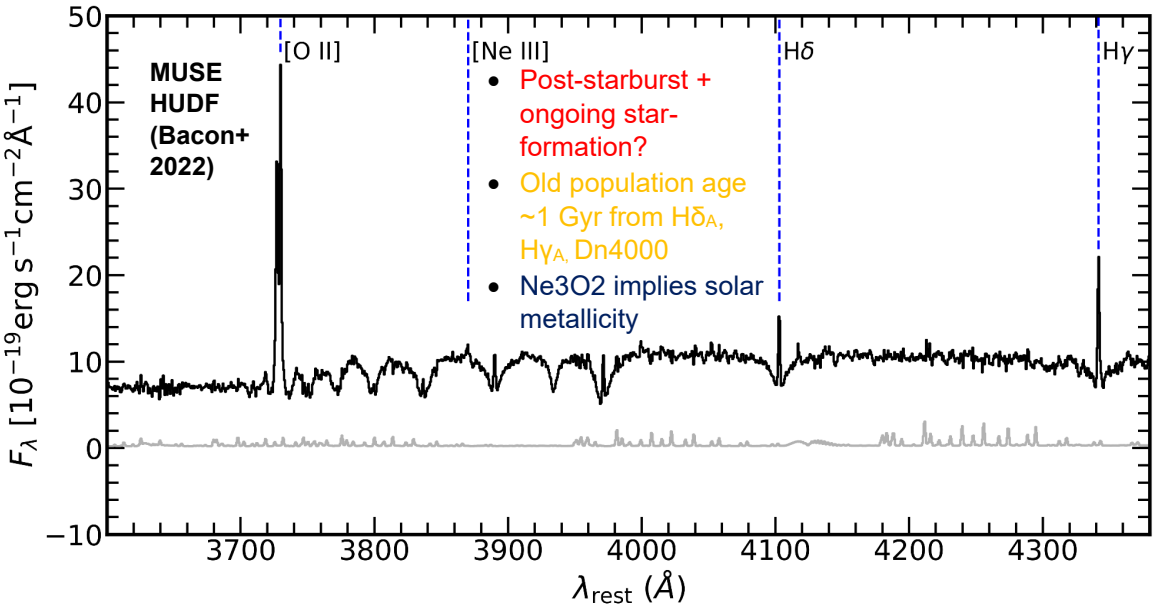

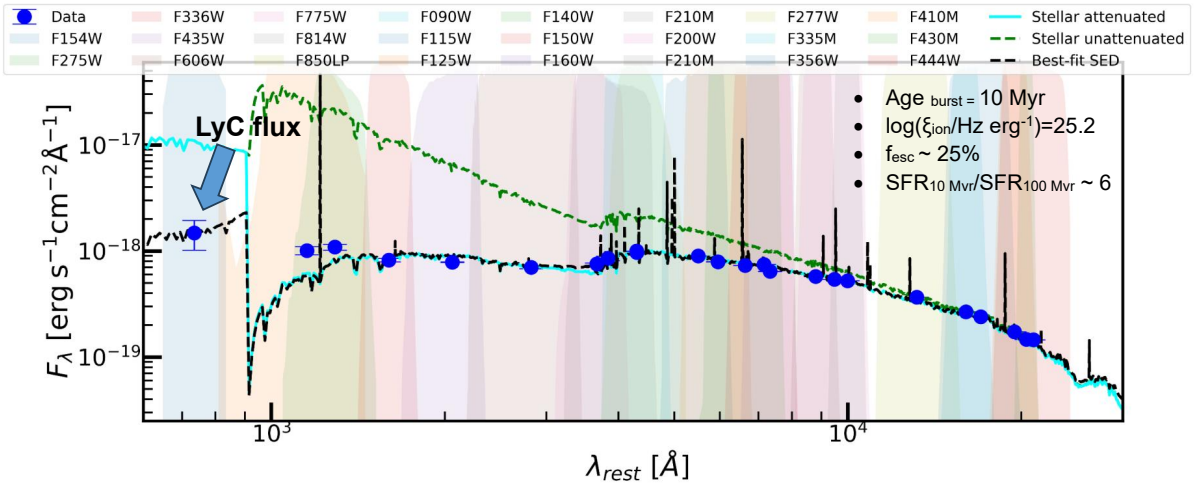

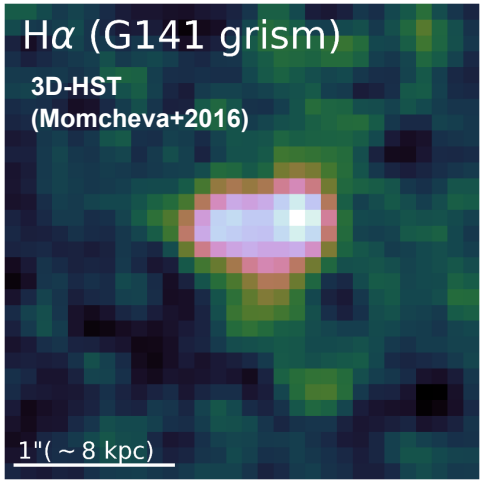

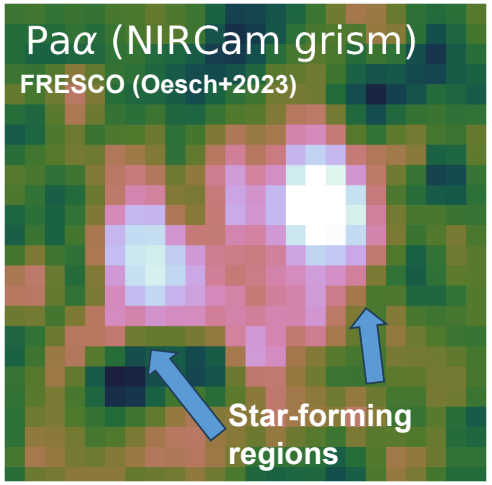

$E(B\text{-}V)_{neb} \sim E(B\text{-}V)_{stellar}$

Ionizing to non-ionizing flux/luminosity ratios

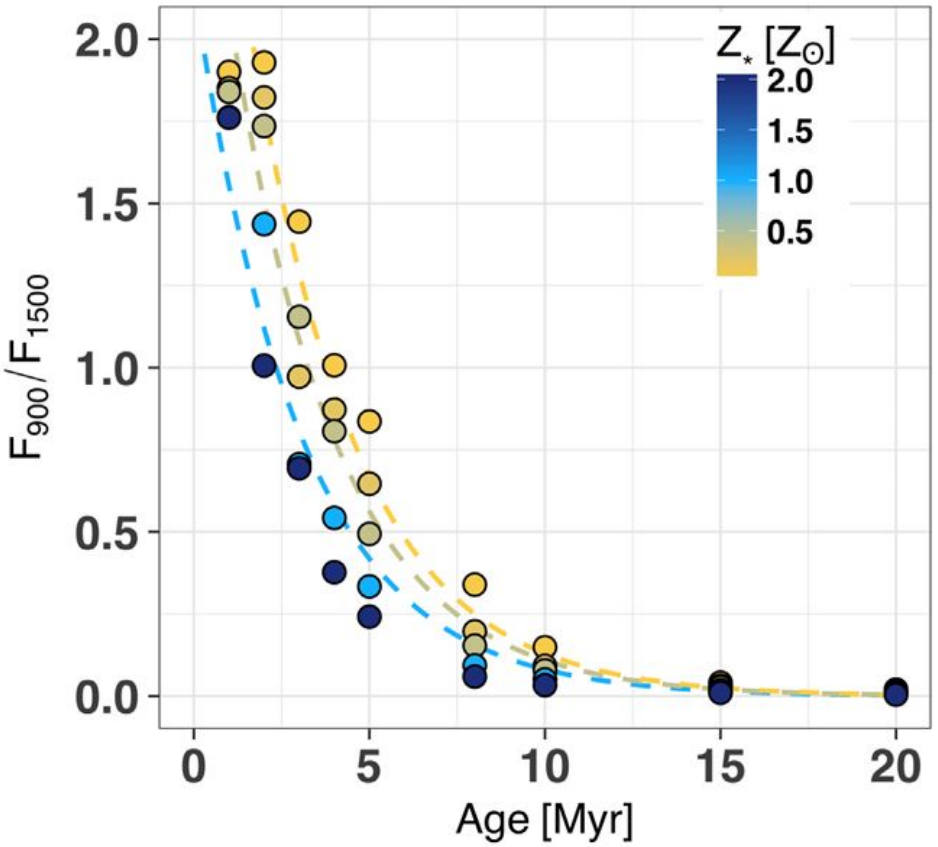

Chisholm+2019

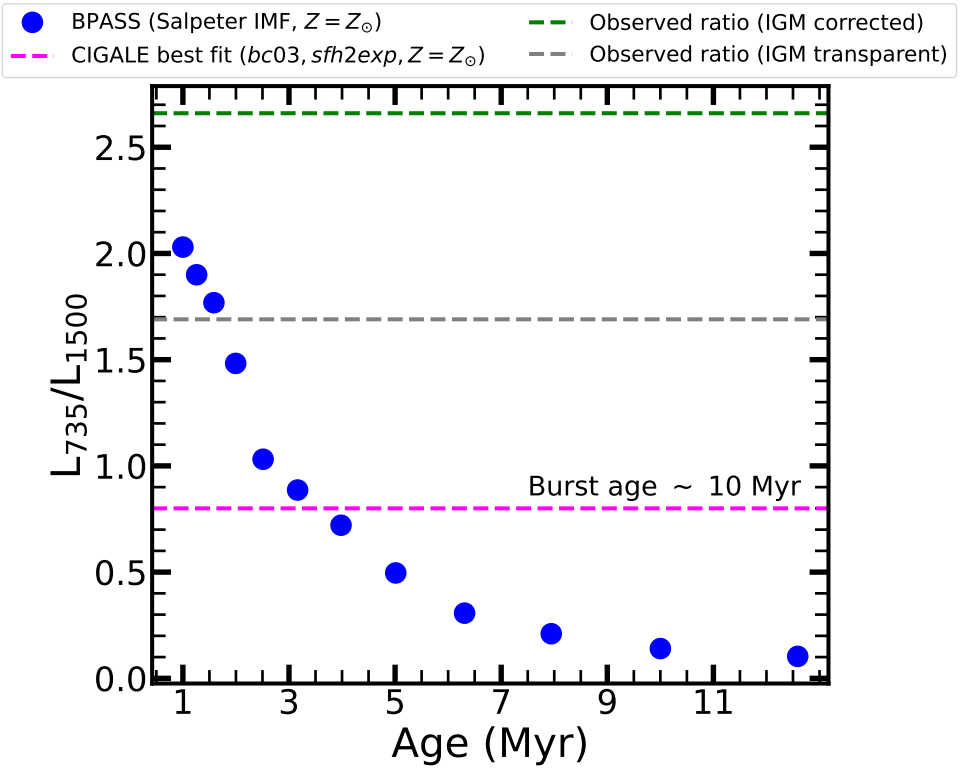

- $(\mathrm{F_{LyC}/F_{1500}})_{\mathrm{obs}} > (\mathrm{L_{LyC}/L_{1500}})_{\mathrm{int}}$.

A possible scenario

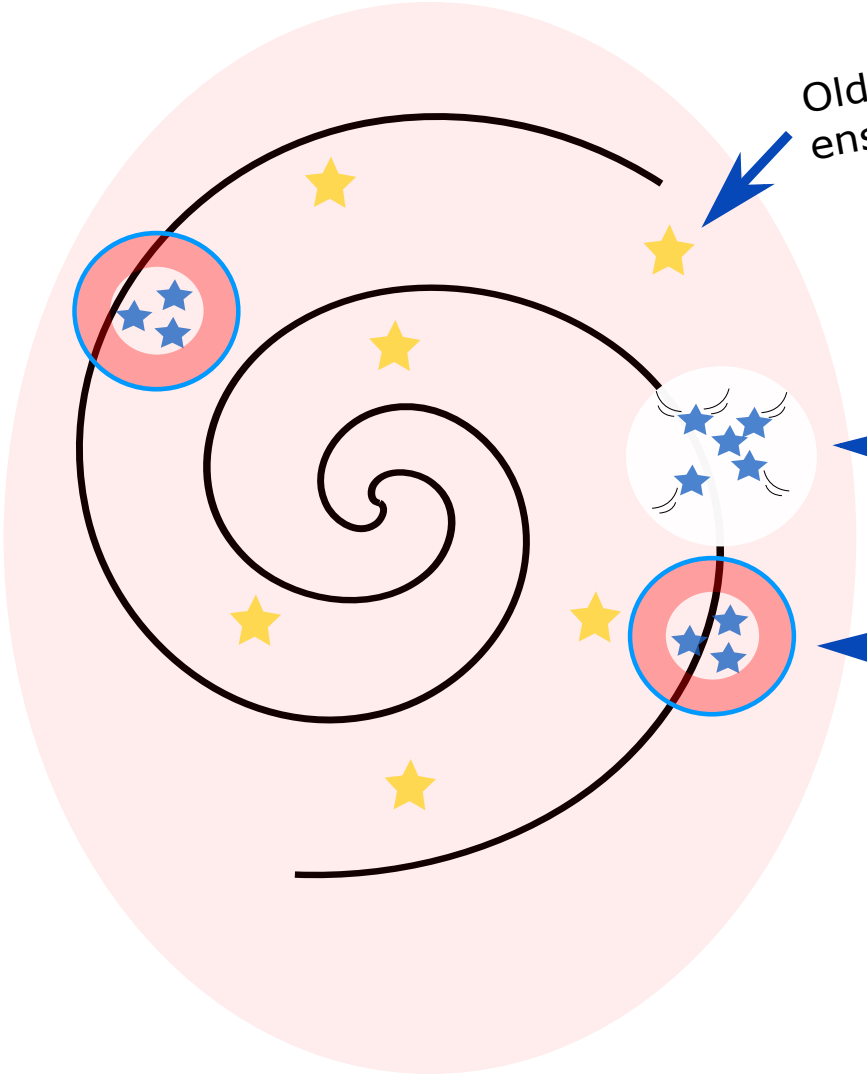

Old stellar population, enshrouded in dust

Site of LyC photons escape, no dust

HII region, LyC photons produced but no escape and enshrouded in dust

$$\left(\frac{F_{735}}{F_{1500}}\right)_{\text{obs, IGM corr}} \sim \frac{f_{esc} \times L_{735}}{L_{1500} \times 10^{-0.4\, A_{1500}}}$$

Outlook

Summary

- Hints of an emerging population of massive dusty LyC leakers.
- A geometry with holes and a complex SFH maybe required to explain the LyC leakage from these class of objects.

Future directions

- Unclear how statistically significant these systems could be to the ionizing budget during the EOR. Including the statistics from non-detections is also important.
- Are the integrated properties good indicators of LyC escape in these cases?
- Could inclination effects play a role as in Lyα escape (Verhamme+2012)?

Properties of LyC leaker candidates at $z \sim 1$ from AUDF surveys

- $f_{esc} \sim 0.15 - 0.85$ and $\log_{10}(\xi_{ion}/\mathrm{Hz\ erg^{-1}}) \sim 25.1 - 25.7$.
- Potential biases from IGM modeling and the depth of the survey though there maybe something more fundamental.

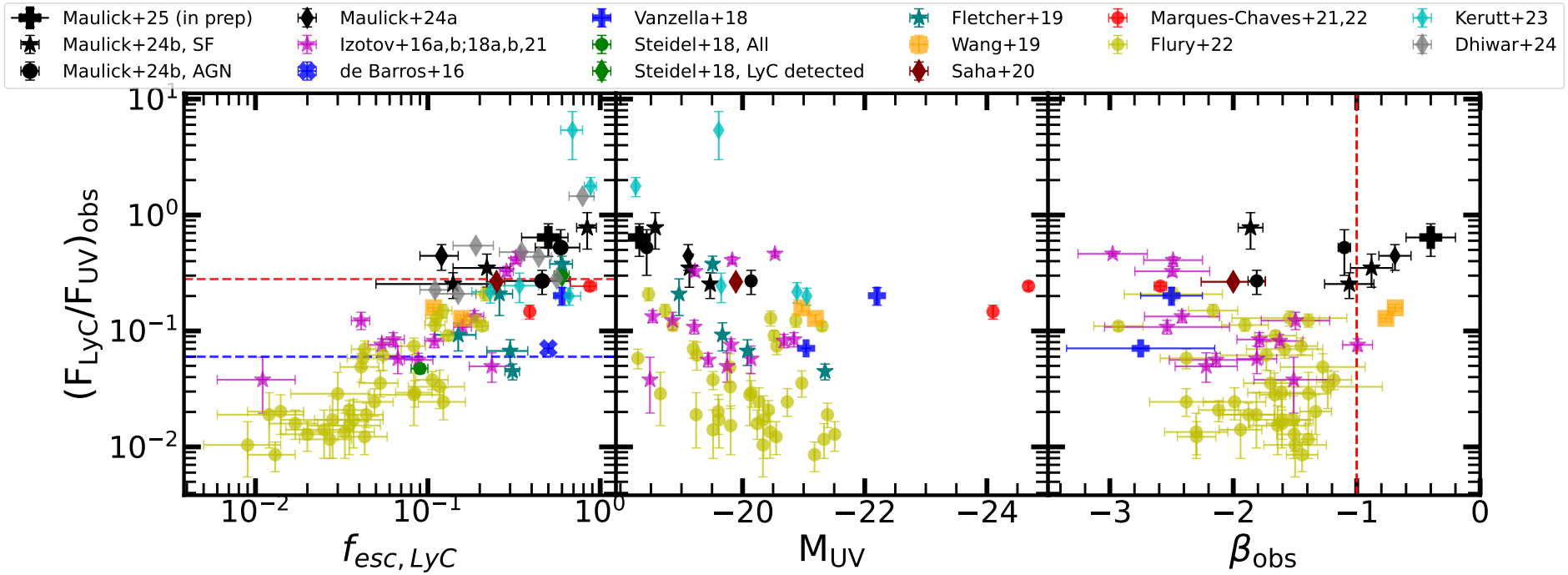

Neutral gas outflows

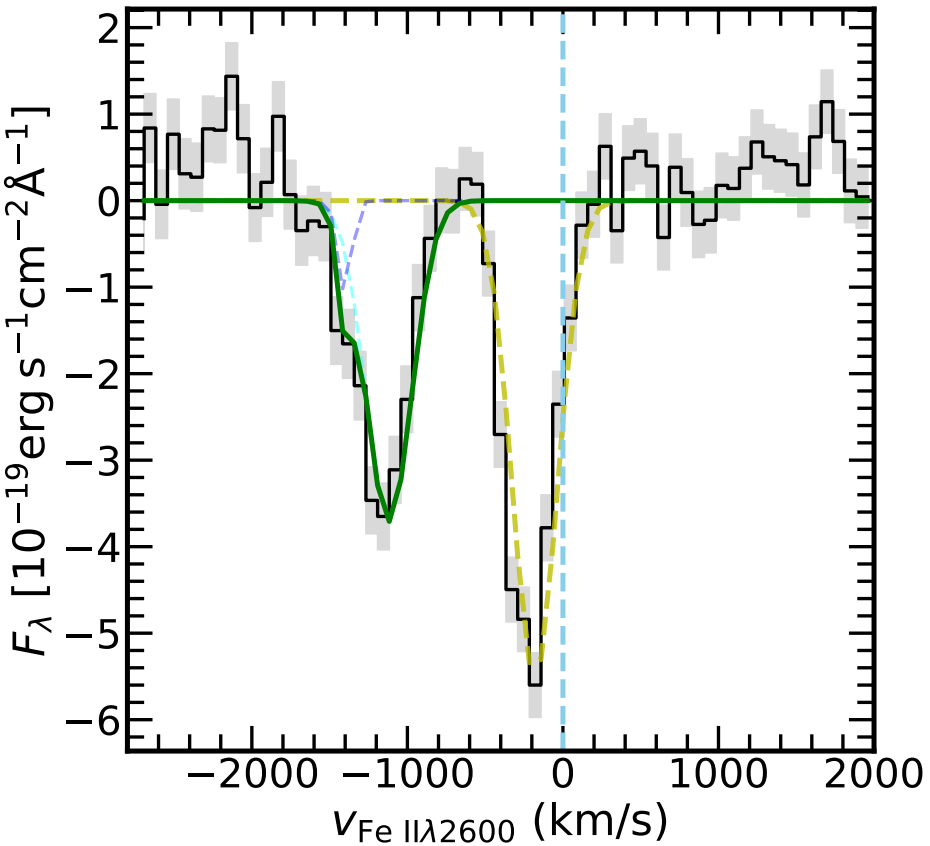

Examples of 'red' LyC leakers at $z \sim 1$ with UVIT (also; Saha+2020 and Dhiwar+2024).

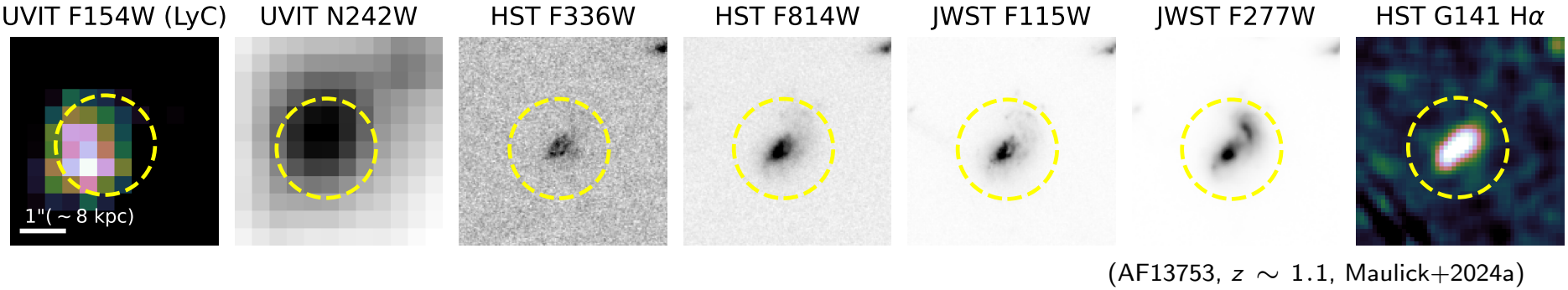

(AF13753, $z \sim 1.1$, Maulick+2024a)

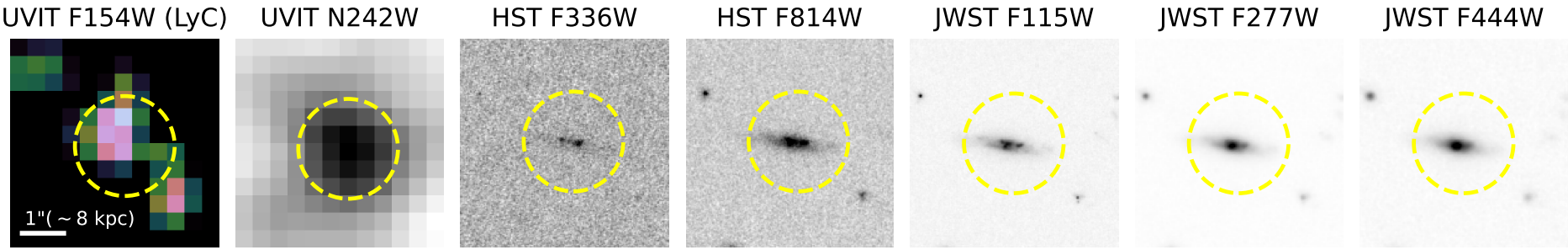

(AUDFs_F14054, $z \sim 0.99$, Maulick+2024b)

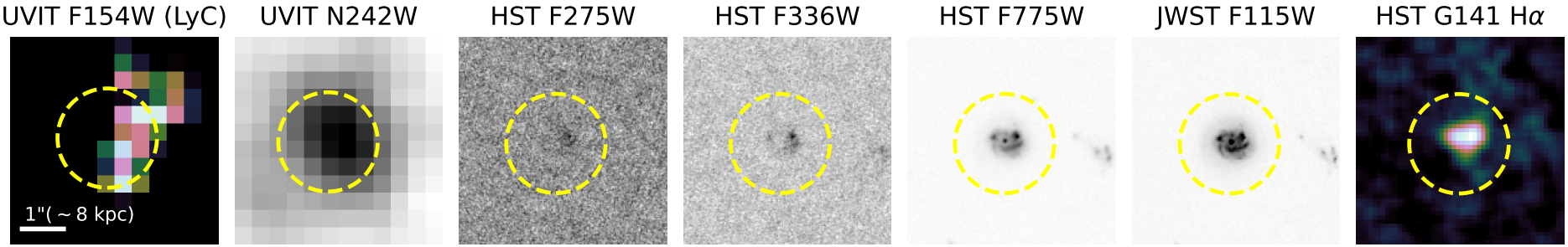

(AUDFs_F15365, $z \sim 1.1$, Maulick+2025, in prep)

Case of LyC Leakage from an Evolved Spiral Galaxy

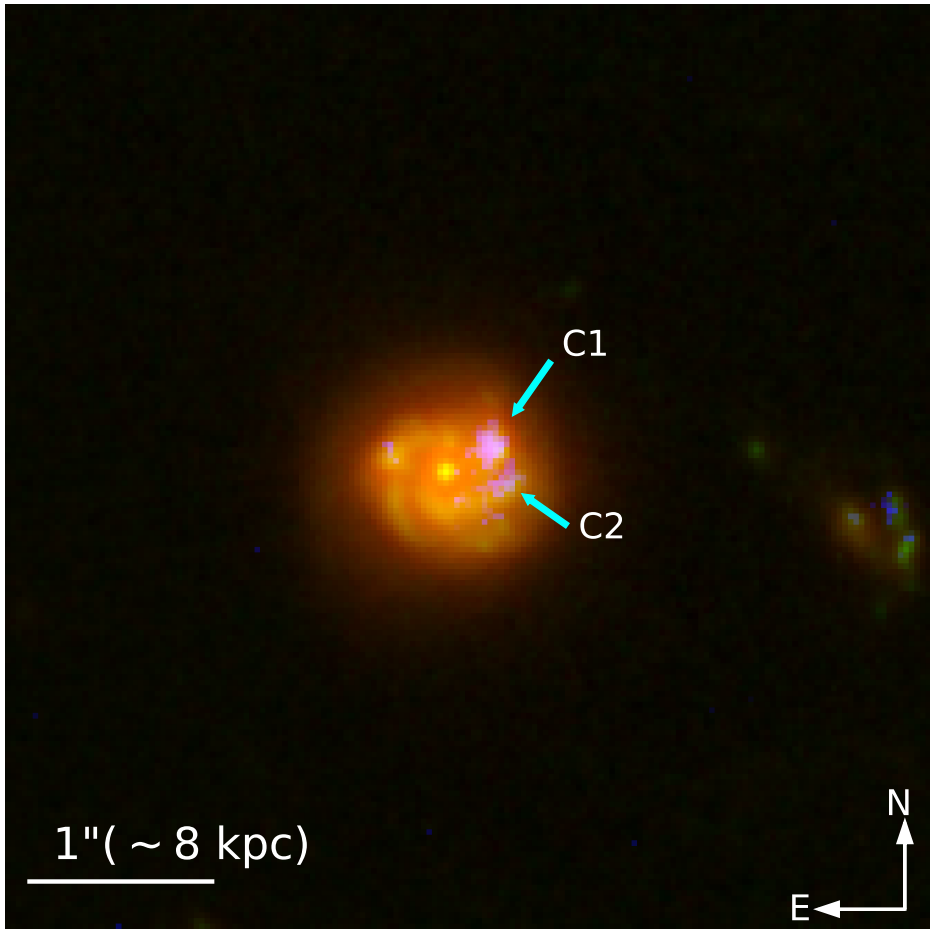

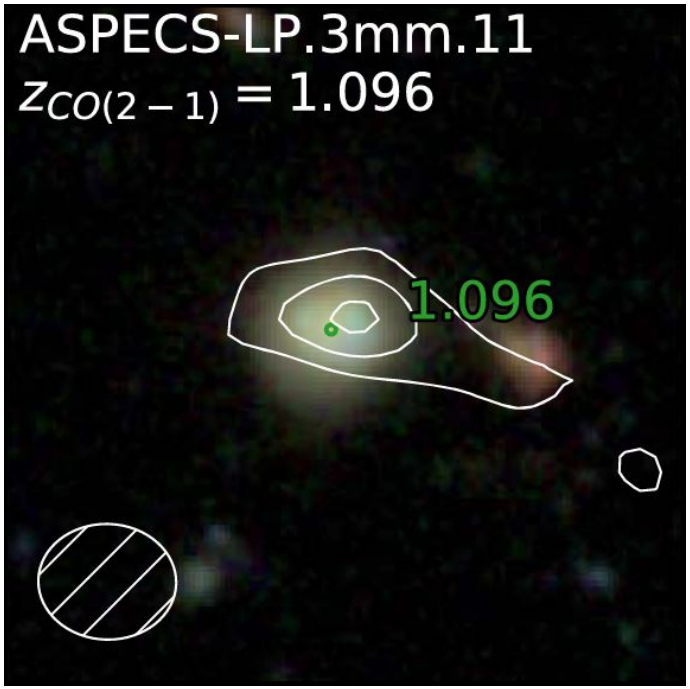

Boogard+2019

- $z \sim 1.1$, located in the HUDF.
- $\log(\mathrm{M}_*/\mathrm{M}_\odot) \sim 10.3$, no X-ray detection.

Overdensity at $z \sim 1.1$

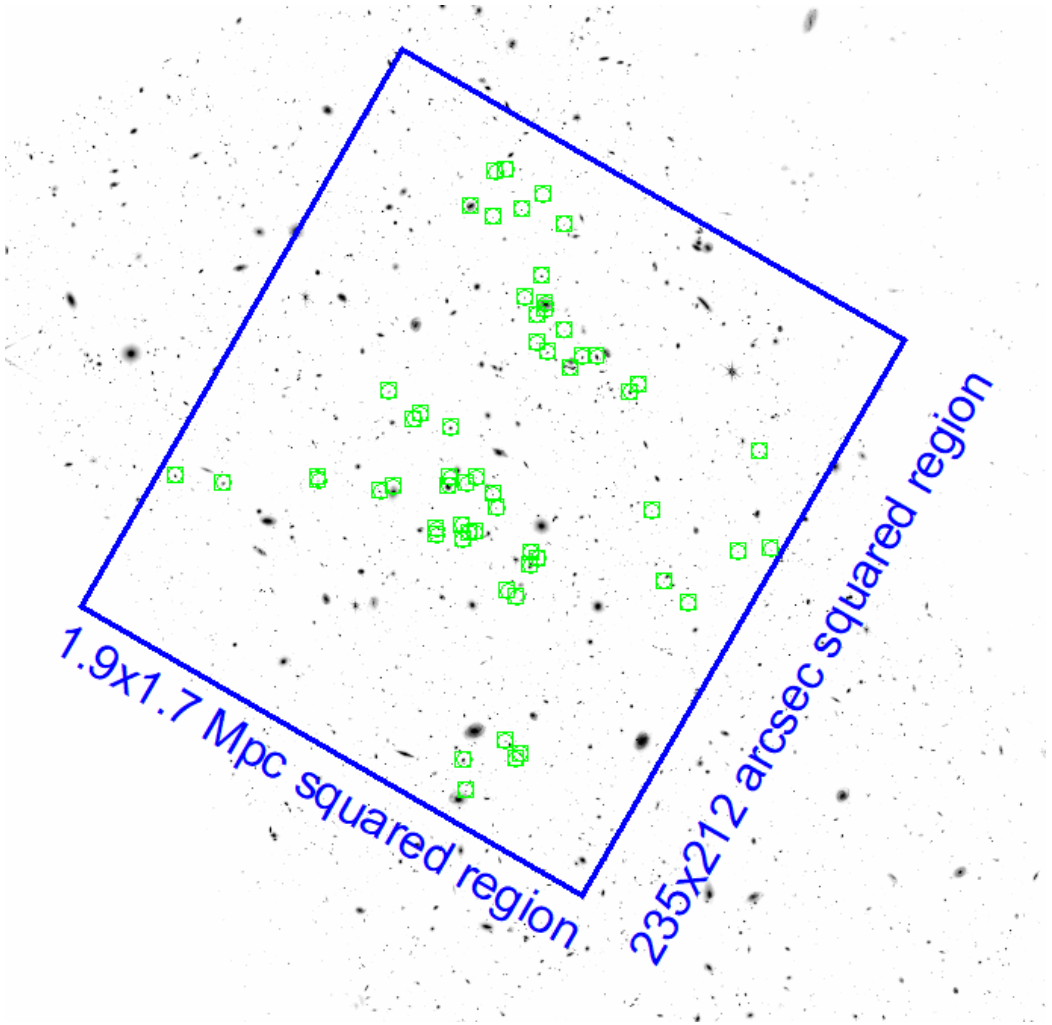

Properties

Properties of AF13753 and Its Individual Components G1 and G2

Column Name	Value
ID (in UVIT F154W catalog)	13753
CANDELS ID	98192
MUSE ID	899
R.A., decl. (J2000)	53.15672, –27.79562
z	1.097
F154W (LyC) S/N	4.15
Hα[1] line flux	90.88 ± 3.18
Hβ line flux	28.53 ± 10.65
Hγ line flux	15.03 ± 0.61
[O III] $\lambda\lambda$4959, 5007 line flux	56.83 ± 5.46
[O II] λ3727 line flux	77.49 ± 0.97
$EW_{H\alpha,rest}$ (Å)	103.12 ± 5.72
$EW_{H\beta,rest}$ (Å)	16.81 ± 6.84
$EW_{[O\ III],rest}$ (Å)	30.79 ± 3.53
Reduced χ^2 of best-fit SED models	0.98 (G1), 0.78 (G2)
$\log_{10}(M_*/M_\odot)$	10.32 ± 0.09 (G1) 10.27 ± 0.10 (G2)
$SFR_{SED,10\ Myr}$ ($M_\odot$ yr^{-1})	33.27 ± 7.09 (G1), 10.37 ± 7.54 (G2)
$SFR_{H\alpha}$ ($M_\odot$ yr^{-1})	47.16 ± 8.71
$E(B-V)_{neb,Balmer}$	0.55 ± 0.02
$E(B-V)_{neb,SED}$	0.5 (G1), 0.5 (G2)
Z_{SED}	0.006 (G1), 0.048 (G2)
$\log_{10}(\xi_{ion}^{H\alpha,case\ B}/\text{Hz erg}^{-1})$ (G1)	25.45 ± 0.10
$\log_{10}(\xi_{ion}^{H\alpha,case\ A}/\text{Hz erg}^{-1})$ (G1)	25.84 ± 0.10
$f_{esc,LyC}^{H\alpha,case\ B}$, $f_{esc,LyC}^{H\alpha,case\ A}$	0.12 ± 0.03 (case B) 0.05 ± 0.01 (case A)
$\bar{f}_{esc,LyC}^{H\alpha,case\ B}$, $\bar{f}_{esc,LyC}^{H\alpha,case\ A}$	0.08 ± 0.02 (case B) 0.03 ± 0.01 (case A)
$f_{esc,SED}$	0.24 ± 0.12 (G1)

Properties

Object	RA (J200)	Dec (J200)	z	LyC detection significance	$f^{1}_{EA>\sigma_{obj}}$	M_{UV}	β_{obs}	$(F_{LyC}/F_{1500})^{2}_{obs}$	$f^{H\alpha\ 2}_{esc,LyC}$	$f^{SED}_{esc,LyC}$	$\log_{10}(\xi/\mathrm{Hz\ erg^{-1}})$	$\log(M_*/M_\odot)$	$SFR^{3}_{SED,10Myr}$ $(M_\odot yr^{-1})$
AUDFs_F20788b	53.0559	-27.7211	1.04	4.30	0.002	-18.57	-1.86 ± 0.10	0.77 ± 0.17	0.84 ± 0.11	0.66 ± 0.14	25.73	8.74 ± 0.20	7.45 ± 3.14
AUDFs_F14054	53.1713	-27.7930	0.99	3.83	0.008	-18.43	-1.36 ± 0.09	0.52 ± 0.14	0.59 ± 0.17	0.70 ± 0.12	25.16	9.23 ± 0.02	4.59 ± 0.20
AUDFs_F21146	53.1129	-27.7199	1.11	3.80	0.009	-19.47	-1.06 ± 0.20	0.25 ± 0.06	0.14 ± 0.09	0.35 ± 0.09	25.14	9.98 ± 0.03	24.60 ± 1.22
AUDFs_F20208	53.1281	-27.7293	1.42	4.05	0.005	-20.14	-1.81 ± 0.06	0.30 ± 0.06	0.46 ± 0.21	0.50 ± 0.06	25.66	9.31 ± 0.11	30.07 ± 3.08
AUDFs_F16775b	53.1588	-27.7706	1.00	3.03	0.034	-19.13	-0.88 ± 0.17	0.34 ± 0.10	0.27 ± 0.10	0.32 ± 0.12	25.12	9.85 ± 0.02	16.94 ± 0.86

Object	CLEAR ID	MUSE ID[1]	$F_{[OII\lambda3727]}$	$F_{H\beta}$	$F^{2}_{[OIII]}$	$F_{H\alpha}$	$EW_{H\beta,rest}$(Å)	$EW_{[OIII],rest}$(Å)	$EW_{H\alpha,rest}$(Å)	$E(B-V)_{neb}$	$SFR^{3}_{H\alpha}$ $(M_\odot yr{-}1)$	Class[4]
AUDFs_F20788b	40553	-	-	2.05 ± 0.42	8.29 ± 0.48	6.15 ± 0.45	$66.22^{+13.57}_{-13.56}$	$214.67^{+14.12}_{-13.66}$	$308.85^{+22.41}_{-24.04}$	0.02 ± 0.26	2.97 ± 1.89	SF
AUDFs_F14054	25304	1002	1.38 ± 0.01	0.18 ± 0.04	1.13 ± 0.05	1.26 ± 0.03	-	-	-	1.02 ± 0.26	6.37 ± 4.09	AGN
AUDFs_F21146	40878	-	-	2.22 ± 0.56	6.14 ± 0.64	15.28 ± 1.07	$16.15^{+3.96}_{-3.94}$	$37.09^{+3.85}_{-4.10}$	$140.02^{+10.38}_{-10.26}$	0.93 ± 0.30	75.96 ± 56.29	SF
AUDFs_F20208	38849	-	-	3.43 ± 1.01	24.30 ± 1.06	2.97 ± 0.66	$61.10^{+18.04}_{-17.93}$	$370.49^{+20.27}_{-19.74}$	$395.07^{+22.30}_{-23.16}$	0.32 ± 0.34	28.53 ± 23.87	AGN
AUDFs_F16775b	30520	13	3.71 ± 0.02	4.22 ± 0.55	4.69 ± 0.58	20.94 ± 0.65	$20.67^{+2.84}_{-2.71}$	$19.07^{+2.30}_{-2.31}$	$139.06^{+4.50}_{-4.61}$	0.54 ± 0.15	30.30 ± 11.25	SF

CIGALE Modules

Module	Parameter	Parameter input
sfh2exp	$\tau^1_{\rm main}$ (Myr)	100,500,1000,1500, 3000,4000
	$\tau^2_{\rm burst}$ (Myr)	50,100,500,1000,2500
	$f^3_{\rm burst}$	0.1,0.2,0.3,0.4,0.5,0.6
	$age^4_{\rm main}$ (Myr)	200,300,500,1000, 1500,2000,3000,5000
	$age^5_{\rm burst}$ (Myr)	2,5,10,20,40,50
bc03	IMF	Salpeter (0)
	metallicity	0.0001,0.0004,0.004, 0.008,0.02
nebular	Gas metallicity	0.0001,0.0004,0.001,0.004, 0.008,0.02
	$f_{\rm esc,LyC}$	0.05,0.1,0.2,0.3,0.4,0.6, 0.7,0.8
	fraction of LyC photons absorbed by dust $f_{\rm dust}$	0,0.1,0.2
Calzetti dust attenuation	$E(B\text{-}V)_{\rm gas}$	0.05,0.15,0.25,0.40, 0.50,0.70,0.90
	E(B-V) factor[7]	0.44
	δ^6	-0.5
	UV bump wavelength	217.5 nm
restframe parameters	UV β slope (Calzetti)	True
	Dn4000[8]	True
	Infrared excess (IRX)	True

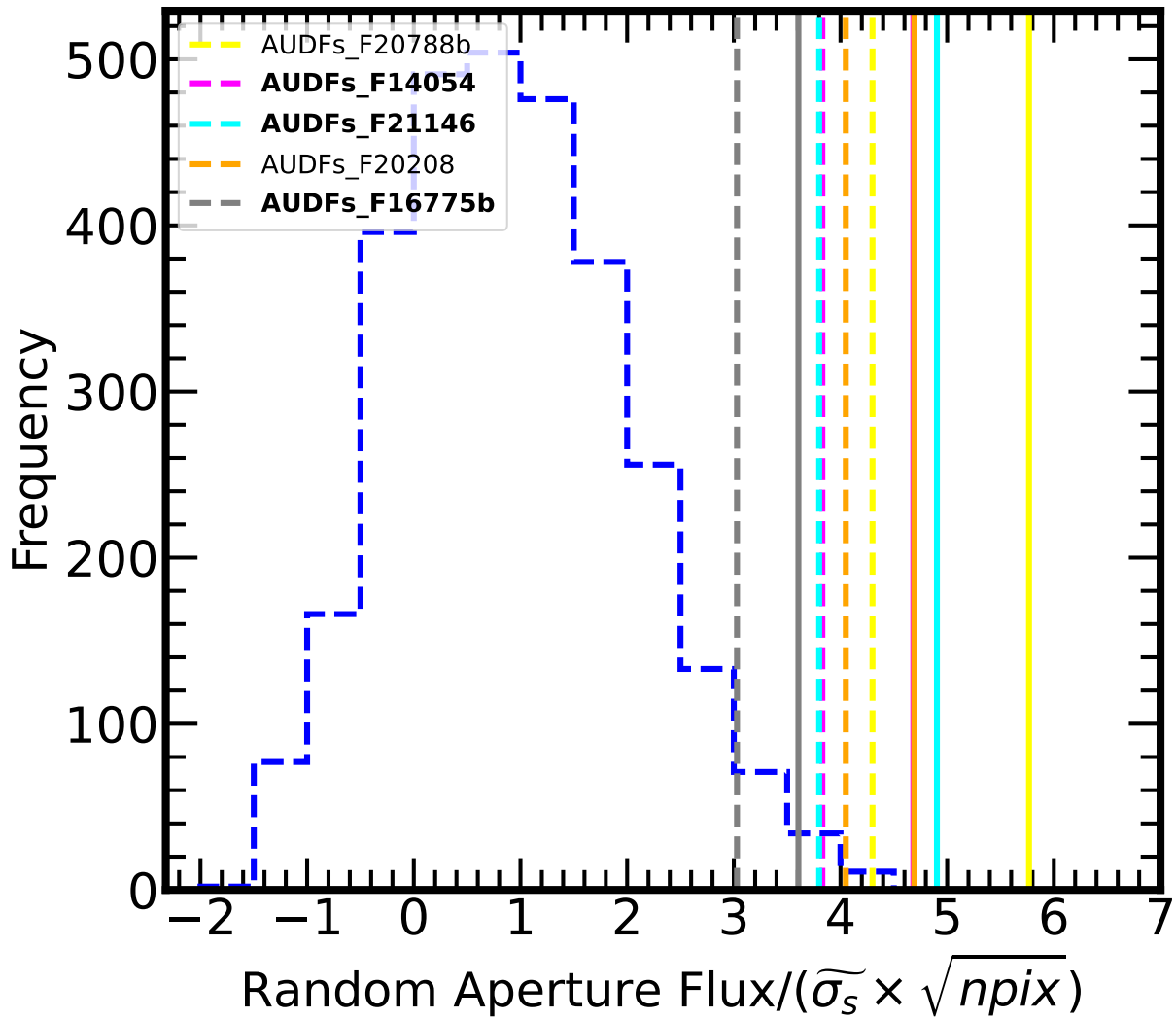
AUDFs_F20788b
AUDFs_F14054
AUDFs_F21146
AUDFs_F20208
AUDFs_F16775b
Frequency
0
100
200
300
400
500
−2
−1
0
1
2
3
4
5
6
7
Random Aperture Flux/($\widetilde{\sigma_s} \times \sqrt{npix}$)

Datasets

- AstroSat UV Deep Field South Survey (AUDF South; Saha, Maulick+2024). Covers ~ 236 arcmin^2. 3σ depth$\sim$ 27.2 (F154W) and 27.7 (N242W).
  - Novel background estimation method (Pandey & Saha, 2024).
  - UVLF at $z \sim 0.4 - 0.8$ (Bhattacharya+2025, in prep).
- High-resolution HST (HLF, Whitaker+2019) and JWST imaging (JADES, Eisenstein+2023, Rieke+2023).
- Slitless spectroscopy (3D-HST, Momcheva+2016; CLEAR, Simons+2023) and MUSE data (Bacon+2022).
- JWST NIRCam grism (FRESCO, Oesch+2023) and JADES NIRSpec (Bunker+2023).

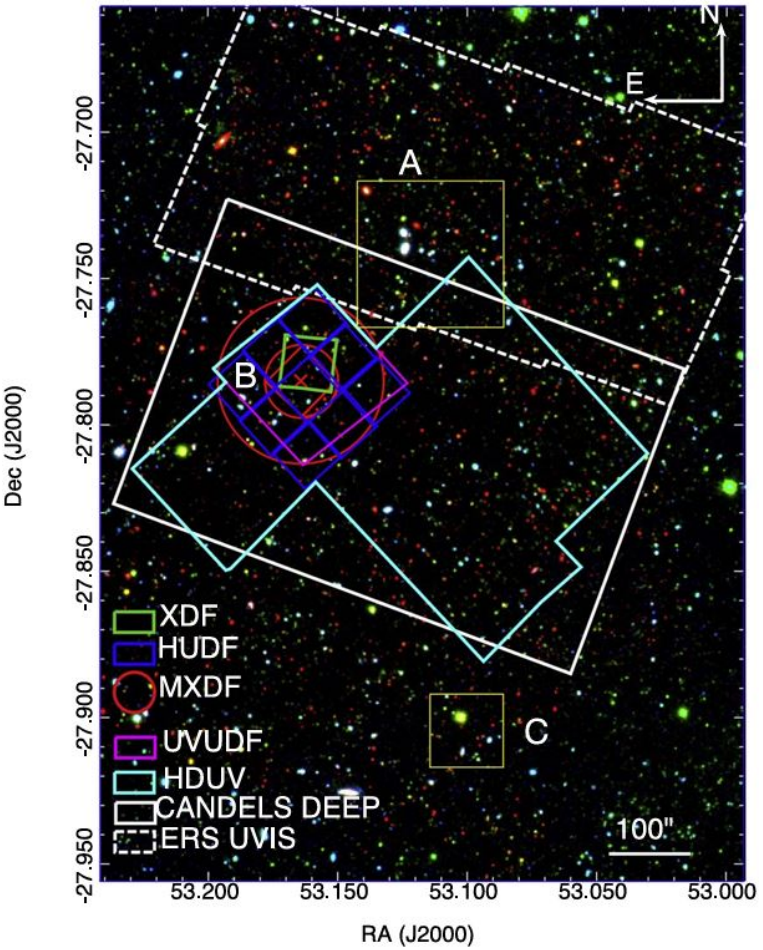

Saha, Maulick+2024

Dusty Massive LyC Leakers, Maulick+2024b